Precision Measurement of the Mass and Lifetime of the Ξ_b^0 Baryon

R. Aaij *et al.*[*]
(LHCb Collaboration)

(Received 28 May 2014; published 15 July 2014)

Using a proton-proton collision data sample corresponding to an integrated luminosity of 3 fb^{-1} collected by LHCb at center-of-mass energies of 7 and 8 TeV, about 3800 $\Xi_b^0 \to \Xi_c^+\pi^-$, $\Xi_c^+ \to pK^-\pi^+$ signal decays are reconstructed. From this sample, the first measurement of the Ξ_b^0 baryon lifetime is made, relative to that of the Λ_b^0 baryon. The mass differences $M(\Xi_b^0) - M(\Lambda_b^0)$ and $M(\Xi_c^+) - M(\Lambda_c^+)$ are also measured with precision more than 4 times better than the current world averages. The resulting values are

$$\frac{\tau_{\Xi_b^0}}{\tau_{\Lambda_b^0}} = 1.006 \pm 0.018 \pm 0.010,$$
$$M(\Xi_b^0) - M(\Lambda_b^0) = 172.44 \pm 0.39 \pm 0.17\ \text{MeV}/c^2,$$
$$M(\Xi_c^+) - M(\Lambda_c^+) = 181.51 \pm 0.14 \pm 0.10\ \text{MeV}/c^2,$$

where the first uncertainty is statistical and the second is systematic. The relative rate of Ξ_b^0 to Λ_b^0 baryon production is measured to be

$$\frac{f_{\Xi_b^0}}{f_{\Lambda_b^0}} \frac{\mathcal{B}(\Xi_b^0 \to \Xi_c^+\pi^-)}{\mathcal{B}(\Lambda_b^0 \to \Lambda_c^+\pi^-)} \frac{\mathcal{B}(\Xi_c^+ \to pK^-\pi^+)}{\mathcal{B}(\Lambda_c^+ \to pK^-\pi^+)} = (1.88 \pm 0.04 \pm 0.03) \times 10^{-2},$$

where the first factor is the ratio of fragmentation fractions, $b \to \Xi_b^0$ relative to $b \to \Lambda_b^0$. Relative production rates as functions of transverse momentum and pseudorapidity are also presented.

DOI: 10.1103/PhysRevLett.113.032001 PACS numbers: 13.30.Eg, 14.20.Mr

Over the past two decades great progress has been made in understanding the nature of hadrons containing beauty quarks. A number of theoretical tools have been developed to describe their decays. One of them, the heavy quark expansion (HQE) [1–8], expresses the decay widths as an expansion in powers of $\Lambda_{\rm QCD}/m_b$, where $\Lambda_{\rm QCD}$ is the energy scale at which the strong coupling constant becomes large and m_b is the b-quark mass. At leading order in the HQE, all weakly decaying b hadrons (excluding those containing charm quarks) have the same lifetime, and differences enter only at order $(\Lambda_{\rm QCD}/m_b)^2$. In the baryon sector, one expects for the lifetimes $\tau(\Xi_b^0) \approx \tau(\Lambda_b^0)$ [8] and $\tau(\Xi_b^0)/\tau(\Xi_b^-) = 0.95 \pm 0.06$ [9,10]. Precise measurements of the Ξ_b^0 and Ξ_b^- lifetimes would put bounds on the magnitude of the higher order terms in the HQE. A number of approaches exist to predict the b-baryon masses [11–19]. As predictions for the masses span a large range, more precise mass measurements will help to refine these models.

Hadron collider experiments have collected large samples of b-baryon decays, which have enabled increasingly precise measurements of their masses and lifetimes [20–25]. These advances include 1% precision on the lifetime of the Λ_b^0 baryon [20] and 0.3 MeV/c^2 uncertainty on its mass [22]. Progress has also been made on improving the precision on the masses of the $\Sigma_b^\pm$ [26], Ξ_b^0 [27–29], Ξ_b^- [26,30], and Ω_b^- [26,30] baryons. The strange-beauty baryon measurements are still limited by small sample sizes owing to their low production rates and either low detection efficiency or small branching fractions.

In this Letter, we present the first measurement of the Ξ_b^0 lifetime and report the most precise measurement of its mass, using a sample of about 3800 $\Xi_b^0 \to \Xi_c^+\pi^-$, $\Xi_c^+ \to pK^-\pi^+$ signal decays. Unless otherwise noted, charge conjugate processes are implied throughout. The $\Lambda_b^0 \to \Lambda_c^+\pi^-$, $\Lambda_c^+ \to pK^-\pi^+$ decay is used for normalization, as it has the same final state and is kinematically very similar. The ratio of Ξ_b^0 to Λ_b^0 baryon production rates, and its dependence on pseudorapidity η and transverse momentum p_T, are also presented. We also use the $\Xi_c^+ \to pK^-\pi^+$ and $\Lambda_c^+ \to pK^-\pi^+$ signals to make the most precise measurement of the Ξ_c^+ mass to date. In what follows, we use X_b (X_c) to refer to either a Ξ_b^0 (Ξ_c^+) or Λ_b^0 (Λ_c^+) baryon.

The measurements use proton-proton (pp) collision data samples collected by the LHCb experiment corresponding

[*] Full author list given at the end of the article.

to an integrated luminosity of 3 fb^{-1}, of which 1 fb^{-1} was recorded at a center-of-mass energy of 7 TeV and 2 fb^{-1} at 8 TeV. The LHCb detector [31] is a single-arm forward spectrometer covering the pseudorapidity range $2 < \eta < 5$, designed for the study of particles containing b or c quarks. The detector includes a high-precision tracking system that provides a momentum measurement with precision of about 0.5% from 2 to 100 GeV/c and impact parameter (IP) resolution of 20 μm for particles with large p_T. Ring-imaging Cherenkov detectors [32] are used to distinguish charged hadrons. Photon, electron, and hadron candidates are identified using a calorimeter system, followed by a set of detectors to identify muons [33].

The trigger [34] consists of a hardware stage, based on information from the calorimeter and muon systems, followed by a software stage, which applies a full event reconstruction [34,35]. About 57% of the recorded X_b events are triggered at the hardware level by one or more of the final state particles in the signal X_b decay. The remaining 43% are triggered only on other activity in the event. We refer to these two classes of events as triggered on signal (TOS) and triggered independently of signal (TIS). The software trigger requires a two-, three-, or four-track secondary vertex with a large sum of the transverse momentum of the particles and a significant displacement from the primary pp interaction vertices (PVs). At least one particle should have $p_T > 1.7$ GeV/c and χ^2_{IP} with respect to any primary interaction greater than 16, where χ^2_{IP} is defined as the difference in χ^2 of a given PV fitted with and without the considered particle included. The signal candidates are required to pass a multivariate software trigger selection algorithm [35].

Proton-proton collisions are simulated using PYTHIA [36] with a specific LHCb configuration [37]. Decays of hadronic particles are described by EVTGEN [38], in which final state radiation is generated using PHOTOS [39]. The interaction of the generated particles with the detector and its response are implemented using the GEANT4 toolkit [40] as described in Ref. [41].

Candidate X_b decays are reconstructed by combining in a kinematic fit selected $X_c \to pK^-\pi^+$ candidates with a π^- candidate (referred to as the bachelor). Each X_b candidate is associated to the PV with the smallest χ^2_{IP}. The X_c daughters are required to have $p_T > 100$ MeV/c, and the bachelor pion is required to have $p_T > 500$ MeV/c. To improve the signal purity, all four final state particles are required to be significantly displaced from the PV and pass particle identification (PID) requirements. The PID requirements on the X_c daughter particles have an efficiency of 74%, while reducing the combinatorial background by a factor of 4. The PID requirements on the bachelor pion are 98% efficient, and remove about 60% of the cross feed from $X_b \to X_cK^-$ decays. Cross feed from misidentified $D^+_{(s)} \to K^+K^-\pi^+$, $D^{*+} \to D^0(K^+K^-)\pi^+$, and $D^+ \to K^-\pi^+\pi^+$ decays is removed by requiring either the mass under these alternate decay hypotheses to be inconsistent with the known $D^{(*)+}_{(s)}$ masses [42] or that the candidate satisfy more stringent PID requirements. The efficiency of these vetoes is about 98% and they reject 28% of the background. The X_c candidate is required to be within 20 MeV/c^2 of the nominal X_c mass [42].

To further improve the signal-to-background ratio, a boosted decision tree (BDT) [43,44] algorithm using eight input variables is employed. Three variables from the X_b candidate are used, χ^2_{IP}, the vertex fit χ^2_{vtx}, and the χ^2_{VS}, which is the increase in χ^2 of the PV fit when the X_b is forced to have zero lifetime relative to the nominal fit. For the X_c baryon, we use the χ^2_{IP}, and among its daughters, we take the minimum p_T, the smallest χ^2_{IP}, and the largest distance between any pair of daughter particles. Finally, the χ^2_{IP} of the bachelor π^- is used. The BDT is trained using simulated signal decays to represent the signal and candidates from the high X_b mass region (beyond the fit region) to describe the background distributions. A selection is applied that provides 97% signal efficiency while rejecting about 50% of the combinatorial background with respect to all previously applied selections.

For each X_b candidate, the mass is recomputed using vertex constraints to improve the momentum resolution; X_c mass constraints are not used since the Ξ_c^+ mass is not known to sufficient precision. The resulting X_b mass spectra are simultaneously fitted to the sum of a signal component and three background contributions. The X_b signal shape is parametrized as the sum of two Crystal Ball functions [45], with a common mean. The shape parameters are freely varied in the fit to data. The Λ_b^0 and Ξ_b^0 signal shape parameters are common except for their means and widths. The Ξ_b^0 widths are fixed to be 0.6% larger than those for the Λ_b^0, based on simulation.

The main background sources are misidentified $X_b \to X_cK^-$ decays, partially reconstructed $X_b \to X_c\rho^-$ and $\Lambda_b^0 \to \Sigma_c^+\pi^-$ decays, and combinatorial background. The $X_b \to X_cK^-$ background shape is obtained from simulated decays that are weighted according to PID misidentification rates obtained from $D^{*+} \to D^0(K^-\pi^+)\pi^+$ calibration data. The $X_b \to X_cK^-$ yield is fixed to be 3.1% of the $X_b \to X_c\pi^-$ signal yield, which is the product of the misidentification rate of 42% and the ratio of branching fractions, $\mathcal{B}(\Lambda_b^0 \to \Lambda_c^+K^-)/\mathcal{B}(\Lambda_b^0 \to \Lambda_c^+\pi^-) = 0.0731 \pm 0.0023$ [27]. The assumed equality of this ratio for Ξ_b^0 and Λ_b^0 is considered as a source of systematic uncertainty. The partially reconstructed backgrounds are modeled empirically using an ARGUS [46] function, convolved with a Gaussian shape; all of its shape parameters are freely varied in the fit. The combinatorial background shape is described using an exponential function with a freely varied shape parameter.

The results of the simultaneous binned extended maximum likelihood fits are shown in Fig. 1. Peaking backgrounds from charmless final states are investigated using the X_c sidebands and are found to be negligible.

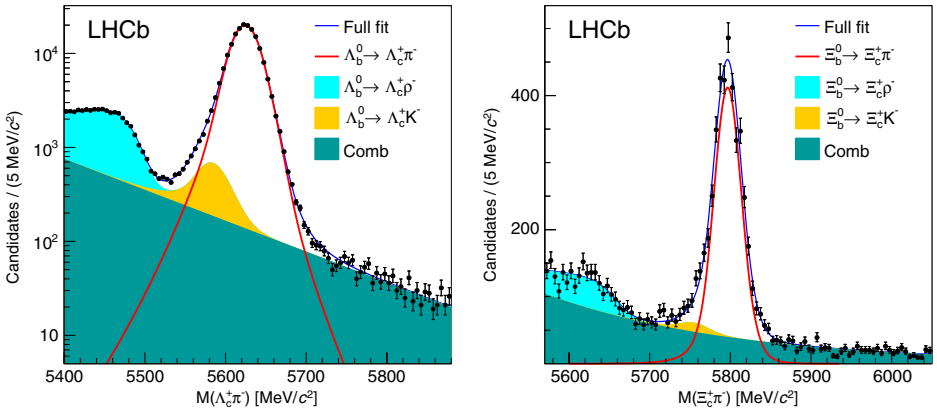

FIG. 1 (color online). Invariant mass spectrum for (left) $\Lambda_b^0 \to \Lambda_c^+\pi^-$ and (right) $\Xi_b^0 \to \Xi_c^+\pi^-$ candidates along with the projections of the fit.

We observe $(180.5 \pm 0.5) \times 10^3$ $\Lambda_b^0 \to \Lambda_c^+\pi^-$ and 3775 ± 71 $\Xi_b^0 \to \Xi_c^+\pi^-$ signal decays. The mass difference is determined to be

$$\Delta M_{X_b} \equiv M(\Xi_b^0) - M(\Lambda_b^0) = 172.44 \pm 0.39\,(\text{stat})\ \text{MeV}/c^2.$$

The data are also used to make the first determination of the relative lifetime $\tau(\Xi_b^0)/\tau(\Lambda_b^0)$. This is performed by fitting the efficiency-corrected ratio of yields, $N_{\text{cor}}(\Xi_b^0)/N_{\text{cor}}(\Lambda_b^0)$, as a function of decay time to an exponential function $e^{\beta t}$. The fitted value of β thus determines $1/\tau_{\Lambda_b^0} - 1/\tau_{\Xi_b^0}$. Since the Λ_b^0 lifetime is known to high precision, $\tau(\Xi_b^0)$ is readily obtained. The data are binned in 0.5 ps bins from 0 to 6 ps, and 1 ps bins from 7 to 9 ps. The same fit as described above for the full sample is used to fit the mass spectra in each time bin. The signal and partially reconstructed background shapes are fixed to the values from the fit to the full data sample, since they do not change with decay time, but the combinatorial background shape is freely varied in each time bin fit.

The measured yield ratio in each time bin is corrected by the relative efficiency, $\epsilon(\Lambda_b^0)/\epsilon(\Xi_b^0)$, as obtained from simulated decays. This ratio is consistent with a constant value of about 0.93, except for the 0.0–0.5 ps bin, which has a value of about 0.7. This lower value is expected due to the differing lifetimes, $\tau(\Xi_c^+) \approx 0.45$ ps $\gg \tau(\Lambda_c^+) \approx 0.2$ ps, and the χ^2_{IP} requirements in the trigger and off-line selections. The 7% overall lower efficiency for the Λ_b^0 mode is due to the larger momenta of the daughters in the Ξ_b^0 decay.

The efficiency-corrected yield ratio is shown in Fig. 2, along with the fit to an exponential function. The points are placed at the weighted average time value within each bin, assuming an exponential distribution with lifetime equal to $\tau(\Lambda_b^0)$. The bias due to this assumption is negligible. From the fit, we find $\beta = (0.40 \pm 1.21) \times 10^{-2}$ ps^{-1}. Using the measured Λ_b^0 lifetime from LHCb of $1.468 \pm 0.009 \pm 0.008$ ps [20], we obtain

$$\frac{\tau_{\Xi_b^0}}{\tau_{\Lambda_b^0}} = \frac{1}{1 - \beta\tau_{\Lambda_b^0}} = 1.006 \pm 0.018\,(\text{stat}),$$

consistent with equal lifetimes of the Ξ_b^0 and Λ_b^0 baryons.

We have also investigated the relative production rates of Ξ_b^0 and Λ_b^0 baryons as functions of p_{T} and η. The p_{T} bin boundaries are 0, 4, 6, 8, 10, 12, 16, 20, up to a maximum of 30 GeV/c, and the η bins are each 0.5 units wide ranging from 2 to 5. The efficiency-corrected yield ratios are shown in Fig. 3. A smooth change in the relative

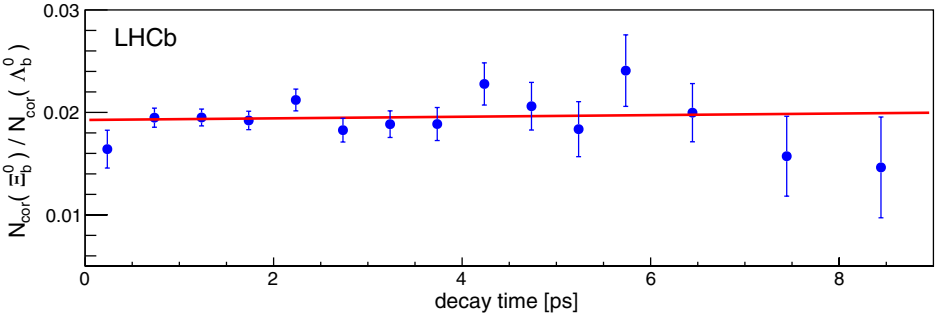

FIG. 2 (color online). Efficiency-corrected yield ratio of $\Xi_b^0 \to \Xi_c^+\pi^-$ relative to $\Lambda_b^0 \to \Lambda_c^+\pi^-$ decays in bins of decay time. A fit using an exponential function is shown. The uncertainties are statistical only.

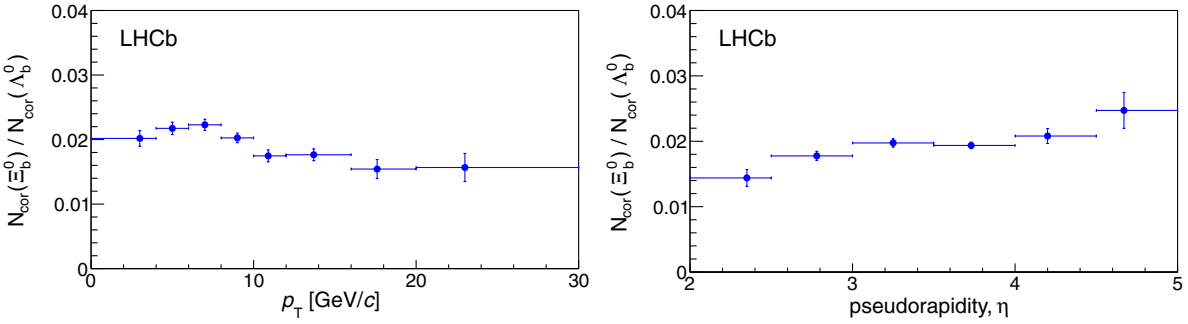

FIG. 3 (color online). Efficiency-corrected yield ratio of $\Xi_b^0 \to \Xi_c^+\pi^-$ relative to $\Lambda_b^0 \to \Lambda_c^+\pi^-$ decays as functions of (left) p_T and (right) pseudorapidity η. The points are positioned along the horizontal axis at the weighted average value within each bin. The uncertainties are statistical only.

production rates, at about the 10%–20% level, is observed. Since the p_T dependence of Ξ_b^0 and Λ_b^0 production are similar, this implies that the steep p_T dependence of Λ_b^0 baryon to B^0 meson production measured in Ref. [47] also occurs for Ξ_b^0 baryons.

The large sample of $\Xi_b^0 \to \Xi_c^+\pi^-$ decays is exploited to measure the Ξ_c^+ mass. Signal X_b candidates within 50 MeV/c^2 of their respective peak values are selected, and a simultaneous fit to the Λ_c^+ and Ξ_c^+ mass spectra is performed. For this measurement, we remove the 20 MeV/c^2 restriction on the X_c mass. The sum of two Crystal Ball functions is used to describe the signal and an exponential shape describes the background. The signal shape parameters are common, except for their means and widths. The larger Ξ_c^+ resolution is due to the greater energy release in the decay. The mass distributions and the results of the fit are shown in Fig. 4. The fitted mass difference is

$$\Delta M_{X_c} \equiv M(\Xi_c^+) - M(\Lambda_c^+) = 181.51 \pm 0.14\,(\text{stat})\ \text{MeV}/c^2.$$

The results presented are all ratio or difference measurements, reducing their sensitivity to most potential biases. A summary of the systematic uncertainties is given in Table I. Unless otherwise noted, systematic uncertainties are assigned by taking the difference between the nominal result and the result after a particular variation. In all measurements, possible dependencies on the signal and background models are investigated by exploring alternative shapes and fit ranges (for mass differences). Uncertainties are combined by summing all sources of uncertainty in quadrature.

For the mass difference measurements, common and separate variations in the fraction of $X_b \to X_c K^-$ by $\pm 1\%$ (absolute) are used to assign the cross-feed uncertainty. Shifts in the momentum scale of $\pm 0.03\%$ [48] are applied coherently to both signal and normalization mode to determine the momentum scale uncertainty. Validation of the procedure on simulated decays shows no biases on the results. The uncertainty due to the limited size of those simulated samples is taken as a systematic error.

For the relative lifetime measurement, the relative acceptance uncertainty is dominated by a potential bias in the first time bin. The uncertainty is assessed by dropping this bin from the fit. Potential bias due to the BDT's usage of χ^2_{IP} information is examined by correcting the data using simulated efficiencies with a tighter BDT requirement. The smaller lifetime of the Λ_b^0 baryon

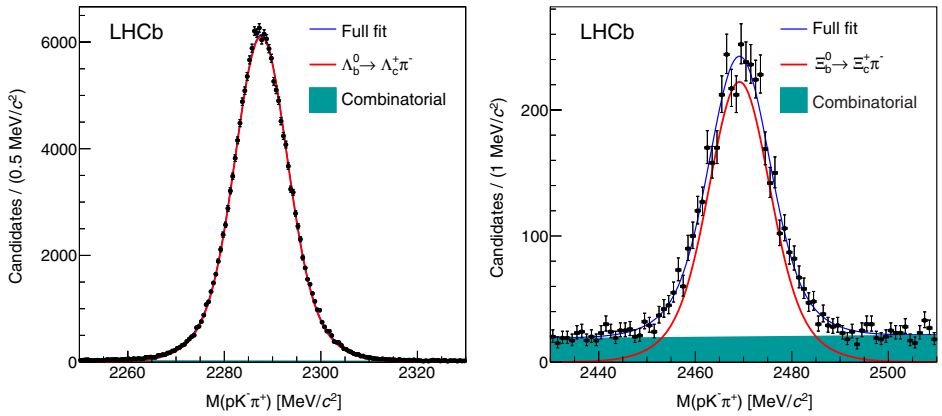

FIG. 4 (color online). Distributions of the $pK^-\pi^+$ invariant mass for (left) Λ_c^+ and (right) Ξ_c^+ candidates along with the projections of the fit.

TABLE I. Summary of systematic uncertainties on the reported measurements. PR represents the relative uncertainty on the production ratio measurement.

Source	ΔM_{X_b} (MeV/c^2)	ΔM_{X_c} (MeV/c^2)	$\tau(\Xi_b^0)/\tau(\Lambda_b^0)$ (%)	PR (%)
Signal and background model	0.06	0.05	0.1	0.5
$X_c K^-$ reflection	0.02	...	...	0.3
Momentum scale	0.06	0.06	...	...
Simulated sample size	0.14	0.07	0.9	0.6
Detection efficiency	...	...	0.4	1.0
BDT requirement	...	...	0.2	...
Trigger	...	...	...	1.3
X_c mass range	...	...	...	0.3
Total	0.17	0.10	1.0	1.9

assumed in the simulation (1.426 ps) has a negligible impact on the measured lifetime ratio. Finally, the finite size of the simulated samples is also taken into account.

For the relative production rate, the signal and background shape uncertainties and the $X_b \to X_c K^-$ cross-feed uncertainties are treated in the same way as above. For the relative acceptance we include contributions from (i) the geometric acceptance by comparing PYTHIA 6 and PYTHIA 8, (ii) the X_c Dalitz structure, by reweighting the efficiencies according to the distributions seen in data, and (iii) the lower efficiency in the 0–0.5 ps bin by requiring $\tau(X_b) > 0.5$ ps. The uncertainty in the relative trigger efficiency is estimated by taking the difference in the average trigger efficiency, when using the different TOS/TIS fractions in data and simulation. A correction and an uncertainty due to the 20 MeV/c^2 mass range on X_c is obtained using the results of the X_c mass fits. The results for the 7 and 8 TeV data differ by about 1% and are statistically compatible with each other.

In summary, a 3 fb^{-1} pp collision data set is used to make the first measurement of the Ξ_b^0 lifetime. The relative and absolute lifetimes are

$$\frac{\tau_{\Xi_b^0}}{\tau_{\Lambda_b^0}} = 1.006 \pm 0.018\,(\text{stat}) \pm 0.010\,(\text{syst}),$$
$$\tau_{\Xi_b^0} = 1.477 \pm 0.026\,(\text{stat}) \pm 0.014\,(\text{syst}) \pm 0.013(\Lambda_b^0)\ \text{ps},$$

where the last uncertainty in $\tau_{\Xi_b^0}$ is due to the precision of $\tau_{\Lambda_b^0}$ [20]. This establishes that the Ξ_b^0 and Λ_b^0 lifetimes are equal to within 2%. We also make the most precise measurements of the mass difference and Ξ_b^0 mass as

$$M(\Xi_b^0) - M(\Lambda_b^0) = 172.44 \pm 0.39\,(\text{stat}) \pm 0.17\,(\text{syst})\ \text{MeV}/c^2,$$
$$M(\Xi_b^0) = 5791.80 \pm 0.39\,(\text{stat}) \pm 0.17\,(\text{syst}) \pm 0.26(\Lambda_b^0)\ \text{MeV}/c^2,$$

where we have used $M(\Lambda_b^0) = 5619.36 \pm 0.26$ MeV/c^2 [22]. The mass and mass difference are consistent with, and about 5 times more precise than, the value recently obtained in Ref. [27].

We also measure the mass difference $M(\Xi_c^+) - M(\Lambda_c^+)$ and the corresponding Ξ_c^+ mass, yielding

$$M(\Xi_c^+) - M(\Lambda_c^+) = 181.51 \pm 0.14\,(\text{stat}) \pm 0.10\,(\text{syst})\ \text{MeV}/c^2,$$
$$M(\Xi_c^+) = 2467.97 \pm 0.14\,(\text{stat}) \pm 0.10\,(\text{syst}) \pm 0.14(\Lambda_c^+)\ \text{MeV}/c^2,$$

where $M(\Lambda_c^+) = 2286.46 \pm 0.14$ MeV/c^2 [42] is used. These values are consistent with and at least 3 times more precise than other measurements [29,42].

Furthermore, the relative yield of Ξ_b^0 and Λ_b^0 baryons as functions of p_T and η are measured, and found to smoothly vary by about 20%. The relative production rate inside the LHCb acceptance is measured to be

$$\frac{f_{\Xi_b^0}}{f_{\Lambda_b^0}} \frac{\mathcal{B}(\Xi_b^0 \to \Xi_c^+ \pi^-)}{\mathcal{B}(\Lambda_b^0 \to \Lambda_c^+ \pi^-)} \frac{\mathcal{B}(\Xi_c^+ \to pK^-\pi^+)}{\mathcal{B}(\Lambda_c^+ \to pK^-\pi^+)} = (1.88 \pm 0.04 \pm 0.03) \times 10^{-2}.$$

The first fraction is the ratio of fragmentation fractions $b \to \Xi_b^0$ relative to $b \to \Lambda_b^0$, and the remainder are branching fractions. Assuming naive Cabibbo factors [49], namely, $\mathcal{B}(\Xi_b^0 \to \Xi_c^+ \pi^-)/\mathcal{B}(\Lambda_b^0 \to \Lambda_c^+ \pi^-) \approx 1$ and $\mathcal{B}(\Xi_c^+ \to pK^-\pi^+)/\mathcal{B}(\Lambda_c^+ \to pK^-\pi^+) \approx 0.1$, one obtains $(f_{\Xi_b^0}/f_{\Lambda_b^0}) \approx 0.2$. The results presented in this Letter provide stringent tests of models that predict the properties of beauty hadrons.

We express our gratitude to our colleagues in the CERN accelerator departments for the excellent performance of the LHC. We thank the technical and administrative staff at the LHCb institutes. We acknowledge support from CERN and from the national agencies: CAPES, CNPq, FAPERJ, and FINEP (Brazil); NSFC (China); CNRS/IN2P3 and Region Auvergne (France); BMBF, DFG, HGF, and MPG (Germany); SFI (Ireland); INFN (Italy); FOM and NWO (Netherlands); SCSR (Poland); MEN/IFA (Romania); MinES, Rosatom, RFBR, and NRC "Kurchatov Institute" (Russia); MinECo, XuntaGal, and GENCAT (Spain); SNSF and SER (Switzerland); NASU (Ukraine);

STFC and the Royal Society (United Kingdom); NSF (U.S.). We also acknowledge the support received from EPLANET, Marie Curie Actions, and the ERC under FP7. The Tier1 computing centers are supported by IN2P3 (France), KIT and BMBF (Germany), INFN (Italy), NWO and SURF (Netherlands), PIC (Spain), GridPP (United Kingdom). We are indebted to the communities behind the multiple open source software packages on which we depend. We are also thankful for the computing resources and the access to software R&D tools provided by Yandex LLC (Russia).

[1] V. A. Khoze and M. A. Shifman, Sov. Phys. Usp. **26**, 387 (1983).
[2] I. I. Bigi and N. Uraltsev, Phys. Lett. B **280**, 271 (1992).
[3] I. I. Bigi, N. G. Uraltsev, and A. I. Vainshtein, Phys. Lett. B **293**, 430 (1992).
[4] B. Blok and M. A. Shifman, Nucl. Phys. **B399**, 441 (1993).
[5] B. Blok and M. A. Shifman, Nucl. Phys. **B399**, 459 (1993).
[6] M. Neubert, Adv. Ser. Dir. High Energy Phys. **15**, 239 (1998).
[7] N. Uraltsev, arXiv:hep-ph/9804275.
[8] I. I. Bigi, arXiv:hep-ph/9508408.
[9] A. J. Lenz, AIP Conf. Proc. **1026**, 36 (2008).
[10] A. J. Lenz, arXiv:1405.3601.
[11] D. Ebert, R. N. Faustov, and V. O. Galkin, Phys. Rev. D **72**, 034026 (2005).
[12] N. Mathur, R. Lewis, and R. M. Woloshyn, Phys. Rev. D **66**, 014502 (2002).
[13] X. Liu, H.-X. Chen, Y.-R. Liu, A. Hosaka, and S.-L. Zhu, Phys. Rev. D **77**, 014031 (2008).
[14] E. E. Jenkins, Phys. Rev. D **77**, 034012 (2008).
[15] R. Roncaglia, D. B. Lichtenberg, and E. Predazzi, Phys. Rev. D **52**, 1722 (1995).
[16] M. Karliner, B. Keren-Zur, H. J. Lipkin, and J. L. Rosner, Ann. Phys. (Amsterdam) **324**, 2 (2009).
[17] M. Karliner, Nucl. Phys. B, Proc. Suppl. **187**, 21 (2009).
[18] Z. Ghalenovi and A. Akbar Rajabi, Eur. Phys. J. Plus **127**, 141 (2012).
[19] J.-R. Zhang and M.-Q. Huang, Phys. Rev. D **78**, 094015 (2008).
[20] R. Aaij *et al.* (LHCb Collaboration), Phys. Lett. B **734**, 122 (2014).
[21] R. Aaij *et al.* (LHCb Collaboration), J. High Energy Phys. 04 (2014) 114.
[22] R. Aaij *et al.* (LHCb Collaboration), Phys. Rev. Lett. **112**, 202001 (2014).
[23] R. Aaij *et al.* (LHCb Collaboration), arXiv:1405.1543.
[24] G. Aad *et al.* (ATLAS Collaboration), Phys. Rev. D **87**, 032002 (2013).
[25] S. Chatrchyan *et al.* (CMS Collaboration), J. High Energy Phys. 07 (2013) 163.
[26] T. Aaltonen *et al.* (CDF Collaboration), Phys. Rev. D **85**, 092011 (2012).
[27] R. Aaij *et al.* (LHCb Collaboration), Phys. Rev. D **89**, 032001 (2014).
[28] T. Aaltonen *et al.* (CDF Collaboration), Phys. Rev. Lett. **107**, 102001 (2011).
[29] T. A. Aaltonen *et al.* (CDF Collaboration), Phys. Rev. D **89**, 072014 (2014).
[30] R. Aaij *et al.* (LHCb Collaboration), Phys. Rev. Lett. **110**, 182001 (2013).
[31] A. A. Alves, Jr. *et al.* (LHCb Collaboration), JINST **3**, S08005 (2008).
[32] M. Adinolfi *et al.*, Eur. Phys. J. C **73**, 2431, (2013).
[33] A. A. Alves, Jr. *et al.*, JINST **8**, P02022 (2013).
[34] R. Aaij *et al.*, JINST **8**, P04022 (2013).
[35] V. V. Gligorov and M. Williams, JINST **8**, P02013 (2013).
[36] T. Sjöstrand, S. Mrenna, and P. Skands, J. High Energy Phys. 05 (2006) 026; Comput. Phys. Commun. **178**, 852 (2008).
[37] I. Belyaev *et al.*, in *Proceedings of the Nuclear Science Symposium Conference (NSS/MIC)* (IEEE, New York, 2010), p. 1155.
[38] D. J. Lange, Nucl. Instrum. Methods Phys. Res., Sect. A **462**, 152 (2001).
[39] P. Golonka and Z. Was, Eur. Phys. J. C **45**, 97 (2006).
[40] J. Allison *et al.* (GEANT4 Collaboration), IEEE Trans. Nucl. Sci. **53**, 270 (2006); S. Agostinelli *et al.* (GEANT4 Collaboration), Nucl. Instrum. Methods Phys. Res., Sect. A **506**, 250 (2003).
[41] M. Clemencic, G. Corti, S. Easo, C. R. Jones, S. Miglioranzi, M. Pappagallo, and P. Robbe, J. Phys. Conf. Ser. **331**, 032023 (2011).
[42] J. Beringer *et al.* (Particle Data Group), Phys. Rev. D **86**, 010001 (2012), and 2013 partial update for the 2014 edition.
[43] L. Breiman, J. H. Friedman, R. A. Olshen, and C. J. Stone, *Classification and Regression Trees* (Wadsworth International Group, Belmont, CA, 1984).
[44] R. E. Schapire and Y. Freund, J. Comput. Syst. Sci. **55**, 119 (1997).
[45] T. Skwarnicki, Ph.D. thesis, Institute of Nuclear Physics, Krakow, 1986 (DESY Report No. DESY-F31-86-02).
[46] H. Albrecht *et al.* (ARGUS Collaboration), Phys. Lett. B **340**, 217 (1994).
[47] R. Aaij *et al.* (LHCb Collaboration), arXiv:1405.6842.
[48] R. Aaij *et al.* (LHCb Collaboration), J. High Energy Phys. 06 (2013) 065.
[49] N. Cabibbo, Phys. Rev. Lett. **10**, 531 (1963).

R. Aaij,[41] B. Adeva,[37] M. Adinolfi,[46] A. Affolder,[52] Z. Ajaltouni,[5] S. Akar,[6] J. Albrecht,[9] F. Alessio,[38] M. Alexander,[51] S. Ali,[41] G. Alkhazov,[30] P. Alvarez Cartelle,[37] A. A. Alves Jr.,[25,38] S. Amato,[2] S. Amerio,[22] Y. Amhis,[7] L. An,[3] L. Anderlini,[17,a] J. Anderson,[40] R. Andreassen,[57] M. Andreotti,[16,b] J. E. Andrews,[58] R. B. Appleby,[54] O. Aquines Gutierrez,[10] F. Archilli,[38] A. Artamonov,[35] M. Artuso,[59] E. Aslanides,[6] G. Auriemma,[25,c] M. Baalouch,[5]

S. Bachmann,[11] J. J. Back,[48] A. Badalov,[36] V. Balagura,[31] W. Baldini,[16] R. J. Barlow,[54] C. Barschel,[38] S. Barsuk,[7] W. Barter,[47] V. Batozskaya,[28] V. Battista,[39] A. Bay,[39] L. Beaucourt,[4] J. Beddow,[51] F. Bedeschi,[23] I. Bediaga,[1] S. Belogurov,[31] K. Belous,[35] I. Belyaev,[31] E. Ben-Haim,[8] G. Bencivenni,[18] S. Benson,[38] J. Benton,[46] A. Berezhnoy,[32] R. Bernet,[40] M.-O. Bettler,[47] M. van Beuzekom,[41] A. Bien,[11] S. Bifani,[45] T. Bird,[54] A. Bizzeti,[17,d] P. M. Bjørnstad,[54] T. Blake,[48] F. Blanc,[39] J. Blouw,[10] S. Blusk,[59] V. Bocci,[25] A. Bondar,[34] N. Bondar,[30,38] W. Bonivento,[15,38] S. Borghi,[54] A. Borgia,[59] M. Borsato,[7] T. J. V. Bowcock,[52] E. Bowen,[40] C. Bozzi,[16] T. Brambach,[9] J. van den Brand,[42] J. Bressieux,[39] D. Brett,[54] M. Britsch,[10] T. Britton,[59] J. Brodzicka,[54] N. H. Brook,[46] H. Brown,[52] A. Bursche,[40] G. Busetto,[22,e] J. Buytaert,[38] S. Cadeddu,[15] R. Calabrese,[16,b] M. Calvi,[20,f] M. Calvo Gomez,[36,g] A. Camboni,[36] P. Campana,[18,38] D. Campora Perez,[38] A. Carbone,[14,h] G. Carboni,[24,i] R. Cardinale,[19,38,j] A. Cardini,[15] H. Carranza-Mejia,[50] L. Carson,[50] K. Carvalho Akiba,[2] G. Casse,[52] L. Cassina,[20] L. Castillo Garcia,[38] M. Cattaneo,[38] Ch. Cauet,[9] R. Cenci,[58] M. Charles,[8] Ph. Charpentier,[38] S. Chen,[54] S.-F. Cheung,[55] N. Chiapolini,[40] M. Chrzaszcz,[40,26] K. Ciba,[38] X. Cid Vidal,[38] G. Ciezarek,[53] P. E. L. Clarke,[50] M. Clemencic,[38] H. V. Cliff,[47] J. Closier,[38] V. Coco,[38] J. Cogan,[6] E. Cogneras,[5] P. Collins,[38] A. Comerma-Montells,[11] A. Contu,[15] A. Cook,[46] M. Coombes,[46] S. Coquereau,[8] G. Corti,[38] M. Corvo,[16,b] I. Counts,[56] B. Couturier,[38] G. A. Cowan,[50] D. C. Craik,[48] M. Cruz Torres,[60] S. Cunliffe,[53] R. Currie,[50] C. D'Ambrosio,[38] J. Dalseno,[46] P. David,[8] P. N. Y. David,[41] A. Davis,[57] K. De Bruyn,[41] S. De Capua,[54] M. De Cian,[11] J. M. De Miranda,[1] L. De Paula,[2] W. De Silva,[57] P. De Simone,[18] D. Decamp,[4] M. Deckenhoff,[9] L. Del Buono,[8] N. Déléage,[4] D. Derkach,[55] O. Deschamps,[5] F. Dettori,[42] A. Di Canto,[38] H. Dijkstra,[38] S. Donleavy,[52] F. Dordei,[11] M. Dorigo,[39] A. Dosil Suárez,[37] D. Dossett,[48] A. Dovbnya,[43] K. Dreimanis,[52] G. Dujany,[54] F. Dupertuis,[39] P. Durante,[38] R. Dzhelyadin,[35] A. Dziurda,[26] A. Dzyuba,[30] S. Easo,[49,38] U. Egede,[53] V. Egorychev,[31] S. Eidelman,[34] S. Eisenhardt,[50] U. Eitschberger,[9] R. Ekelhof,[9] L. Eklund,[51,38] I. El Rifai,[5] Ch. Elsasser,[40] S. Ely,[59] S. Esen,[11] H.-M. Evans,[47] T. Evans,[55] A. Falabella,[16,b] C. Färber,[11] C. Farinelli,[41] N. Farley,[45] S. Farry,[52] D. Ferguson,[50] V. Fernandez Albor,[37] F. Ferreira Rodrigues,[1] M. Ferro-Luzzi,[38] S. Filippov,[33] M. Fiore,[16,b] M. Fiorini,[16,b] M. Firlej,[27] C. Fitzpatrick,[38] T. Fiutowski,[27] M. Fontana,[10] F. Fontanelli,[19,j] R. Forty,[38] O. Francisco,[2] M. Frank,[38] C. Frei,[38] M. Frosini,[17,38,a] J. Fu,[21,38] E. Furfaro,[24,i] A. Gallas Torreira,[37] D. Galli,[14,h] S. Gallorini,[22] S. Gambetta,[19,j] M. Gandelman,[2] P. Gandini,[59] Y. Gao,[3] J. Garofoli,[59] J. Garra Tico,[47] L. Garrido,[36] C. Gaspar,[38] R. Gauld,[55] L. Gavardi,[9] G. Gavrilov,[30] E. Gersabeck,[11] M. Gersabeck,[54] T. Gershon,[48] Ph. Ghez,[4] A. Gianelle,[22] S. Giani',[39] V. Gibson,[47] L. Giubega,[29] V. V. Gligorov,[38] C. Göbel,[60] D. Golubkov,[31] A. Golutvin,[53,31,38] A. Gomes,[1,k] H. Gordon,[38] C. Gotti,[20] M. Grabalosa Gándara,[5] R. Graciani Diaz,[36] L. A. Granado Cardoso,[38] E. Graugés,[36] G. Graziani,[17] A. Grecu,[29] E. Greening,[55] S. Gregson,[47] P. Griffith,[45] L. Grillo,[11] O. Grünberg,[62] B. Gui,[59] E. Gushchin,[33] Yu. Guz,[35,38] T. Gys,[38] C. Hadjivasiliou,[59] G. Haefeli,[39] C. Haen,[38] S. C. Haines,[47] S. Hall,[53] B. Hamilton,[58] T. Hampson,[46] X. Han,[11] S. Hansmann-Menzemer,[11] N. Harnew,[55] S. T. Harnew,[46] J. Harrison,[54] T. Hartmann,[62] J. He,[38] T. Head,[38] V. Heijne,[41] K. Hennessy,[52] P. Henrard,[5] L. Henry,[8] J. A. Hernando Morata,[37] E. van Herwijnen,[38] M. Heß,[62] A. Hicheur,[1] D. Hill,[55] M. Hoballah,[5] C. Hombach,[54] W. Hulsbergen,[41] P. Hunt,[55] N. Hussain,[55] D. Hutchcroft,[52] D. Hynds,[51] M. Idzik,[27] P. Ilten,[56] R. Jacobsson,[38] A. Jaeger,[11] J. Jalocha,[55] E. Jans,[41] P. Jaton,[39] A. Jawahery,[58] F. Jing,[3] M. John,[55] D. Johnson,[55] C. R. Jones,[47] C. Joram,[38] B. Jost,[38] N. Jurik,[59] M. Kaballo,[9] S. Kandybei,[43] W. Kanso,[6] M. Karacson,[38] T. M. Karbach,[38] S. Karodia,[51] M. Kelsey,[59] I. R. Kenyon,[45] T. Ketel,[42] B. Khanji,[20] C. Khurewathanakul,[39] S. Klaver,[54] O. Kochebina,[7] M. Kolpin,[11] I. Komarov,[39] R. F. Koopman,[42] P. Koppenburg,[41,38] M. Korolev,[32] A. Kozlinskiy,[41] L. Kravchuk,[33] K. Kreplin,[11] M. Kreps,[48] G. Krocker,[11] P. Krokovny,[34] F. Kruse,[9] W. Kucewicz,[26,l] M. Kucharczyk,[20,26,38,f] V. Kudryavtsev,[34] K. Kurek,[28] T. Kvaratskheliya,[31] V. N. La Thi,[39] D. Lacarrere,[38] G. Lafferty,[54] A. Lai,[15] D. Lambert,[50] R. W. Lambert,[42] E. Lanciotti,[38] G. Lanfranchi,[18] C. Langenbruch,[38] B. Langhans,[38] T. Latham,[48] C. Lazzeroni,[45] R. Le Gac,[6] J. van Leerdam,[41] J.-P. Lees,[4] R. Lefèvre,[5] A. Leflat,[32] J. Lefrançois,[7] S. Leo,[23] O. Leroy,[6] T. Lesiak,[26] B. Leverington,[11] Y. Li,[3] M. Liles,[52] R. Lindner,[38] C. Linn,[38] F. Lionetto,[40] B. Liu,[15] G. Liu,[38] S. Lohn,[38] I. Longstaff,[51] J. H. Lopes,[2] N. Lopez-March,[39] P. Lowdon,[40] H. Lu,[3] D. Lucchesi,[22,e] H. Luo,[50] A. Lupato,[22] E. Luppi,[16,b] O. Lupton,[55] F. Machefert,[7] I. V. Machikhiliyan,[31] F. Maciuc,[29] O. Maev,[30] S. Malde,[55] G. Manca,[15,m] G. Mancinelli,[6] J. Maratas,[5] J. F. Marchand,[4] U. Marconi,[14] C. Marin Benito,[36] P. Marino,[23,n] R. Märki,[39] J. Marks,[11] G. Martellotti,[25] A. Martens,[8] A. Martín Sánchez,[7] M. Martinelli,[41] D. Martinez Santos,[42] F. Martinez Vidal,[64] D. Martins Tostes,[2] A. Massafferri,[1] R. Matev,[38] Z. Mathe,[38] C. Matteuzzi,[20] A. Mazurov,[16,b] M. McCann,[53] J. McCarthy,[45] A. McNab,[54] R. McNulty,[12] B. McSkelly,[52] B. Meadows,[57] F. Meier,[9] M. Meissner,[11] M. Merk,[41] D. A. Milanes,[8] M.-N. Minard,[4] N. Moggi,[14] J. Molina Rodriguez,[60] S. Monteil,[5] M. Morandin,[22] P. Morawski,[27] A. Mordà,[6] M. J. Morello,[23,n] J. Moron,[27] A.-B. Morris,[50] R. Mountain,[59] F. Muheim,[50] K. Müller,[40] R. Muresan,[29] M. Mussini,[14] B. Muster,[39] P. Naik,[46] T. Nakada,[39]

R. Nandakumar,[49] I. Nasteva,[2] M. Needham,[50] N. Neri,[21] S. Neubert,[38] N. Neufeld,[38] M. Neuner,[11] A. D. Nguyen,[39] T. D. Nguyen,[39] C. Nguyen-Mau,[39,o] M. Nicol,[7] V. Niess,[5] R. Niet,[9] N. Nikitin,[32] T. Nikodem,[11] A. Novoselov,[35] D. P. O'Hanlon,[48] A. Oblakowska-Mucha,[27] V. Obraztsov,[35] S. Oggero,[41] S. Ogilvy,[51] O. Okhrimenko,[44] R. Oldeman,[15,m] G. Onderwater,[65] M. Orlandea,[29] J. M. Otalora Goicochea,[2] P. Owen,[53] A. Oyanguren,[64] B. K. Pal,[59] A. Palano,[13,p] F. Palombo,[21,q] M. Palutan,[18] J. Panman,[38] A. Papanestis,[49,38] M. Pappagallo,[51] C. Parkes,[54] C. J. Parkinson,[9,45] G. Passaleva,[17] G. D. Patel,[52] M. Patel,[53] C. Patrignani,[19,j] A. Pazos Alvarez,[37] A. Pearce,[54] A. Pellegrino,[41] M. Pepe Altarelli,[38] S. Perazzini,[14,h] E. Perez Trigo,[37] P. Perret,[5] M. Perrin-Terrin,[6] L. Pescatore,[45] E. Pesen,[66] K. Petridis,[53] A. Petrolini,[19,j] E. Picatoste Olloqui,[36] B. Pietrzyk,[4] T. Pilař,[48] D. Pinci,[25] A. Pistone,[19] S. Playfer,[50] M. Plo Casasus,[37] F. Polci,[8] A. Poluektov,[48,34] E. Polycarpo,[2] A. Popov,[35] D. Popov,[10] B. Popovici,[29] C. Potterat,[2] E. Price,[46] J. Prisciandaro,[39] A. Pritchard,[52] C. Prouve,[46] V. Pugatch,[44] A. Puig Navarro,[39] G. Punzi,[23,r] W. Qian,[4] B. Rachwal,[26] J. H. Rademacker,[46] B. Rakotomiaramanana,[39] M. Rama,[18] M. S. Rangel,[2] I. Raniuk,[43] N. Rauschmayr,[38] G. Raven,[42] S. Reichert,[54] M. M. Reid,[48] A. C. dos Reis,[1] S. Ricciardi,[49] S. Richards,[46] M. Rihl,[38] K. Rinnert,[52] V. Rives Molina,[36] D. A. Roa Romero,[5] P. Robbe,[7] A. B. Rodrigues,[1] E. Rodrigues,[54] P. Rodriguez Perez,[54] S. Roiser,[38] V. Romanovsky,[35] A. Romero Vidal,[37] M. Rotondo,[22] J. Rouvinet,[39] T. Ruf,[38] F. Ruffini,[23] H. Ruiz,[36] P. Ruiz Valls,[64] G. Sabatino,[25,i] J. J. Saborido Silva,[37] N. Sagidova,[30] P. Sail,[51] B. Saitta,[15,m] V. Salustino Guimaraes,[2] C. Sanchez Mayordomo,[64] B. Sanmartin Sedes,[37] R. Santacesaria,[25] C. Santamarina Rios,[37] E. Santovetti,[24,i] M. Sapunov,[6] A. Sarti,[18,s] C. Satriano,[25,c] A. Satta,[24] D. M. Saunders,[46] M. Savrie,[16,b] D. Savrina,[31,32] M. Schiller,[42] H. Schindler,[38] M. Schlupp,[9] M. Schmelling,[10] B. Schmidt,[38] O. Schneider,[39] A. Schopper,[38] M.-H. Schune,[7] R. Schwemmer,[38] B. Sciascia,[18] A. Sciubba,[25] M. Seco,[37] A. Semennikov,[31] I. Sepp,[53] N. Serra,[40] J. Serrano,[6] L. Sestini,[22] P. Seyfert,[11] M. Shapkin,[35] I. Shapoval,[16,43,b] Y. Shcheglov,[30] T. Shears,[52] L. Shekhtman,[34] V. Shevchenko,[63] A. Shires,[9] R. Silva Coutinho,[48] G. Simi,[22] M. Sirendi,[47] N. Skidmore,[46] T. Skwarnicki,[59] N. A. Smith,[52] E. Smith,[55,49] E. Smith,[53] J. Smith,[47] M. Smith,[54] H. Snoek,[41] M. D. Sokoloff,[57] F. J. P. Soler,[51] F. Soomro,[39] D. Souza,[46] B. Souza De Paula,[2] B. Spaan,[9] A. Sparkes,[50] P. Spradlin,[51] F. Stagni,[38] M. Stahl,[11] S. Stahl,[11] O. Steinkamp,[40] O. Stenyakin,[35] S. Stevenson,[55] S. Stoica,[29] S. Stone,[59] B. Storaci,[40] S. Stracka,[23,38] M. Straticiuc,[29] U. Straumann,[40] R. Stroili,[22] V. K. Subbiah,[38] L. Sun,[57] W. Sutcliffe,[53] K. Swientek,[27] S. Swientek,[9] V. Syropoulos,[42] M. Szczekowski,[28] P. Szczypka,[39,38] D. Szilard,[2] T. Szumlak,[27] S. T'Jampens,[4] M. Teklishyn,[7] G. Tellarini,[16,b] F. Teubert,[38] C. Thomas,[55] E. Thomas,[38] J. van Tilburg,[41] V. Tisserand,[4] M. Tobin,[39] S. Tolk,[42] L. Tomassetti,[16,b] D. Tonelli,[38] S. Topp-Joergensen,[55] N. Torr,[55] E. Tournefier,[4] S. Tourneur,[39] M. T. Tran,[39] M. Tresch,[40] A. Tsaregorodtsev,[6] P. Tsopelas,[41] N. Tuning,[41] M. Ubeda Garcia,[38] A. Ukleja,[28] A. Ustyuzhanin,[63] U. Uwer,[11] V. Vagnoni,[14] G. Valenti,[14] A. Vallier,[7] R. Vazquez Gomez,[18] P. Vazquez Regueiro,[37] C. Vázquez Sierra,[37] S. Vecchi,[16] J. J. Velthuis,[46] M. Veltri,[17,t] G. Veneziano,[39] M. Vesterinen,[11] B. Viaud,[7] D. Vieira,[2] M. Vieites Diaz,[37] X. Vilasis-Cardona,[36,g] A. Vollhardt,[40] D. Volyanskyy,[10] D. Voong,[46] A. Vorobyev,[30] V. Vorobyev,[34] C. Voß,[62] H. Voss,[10] J. A. de Vries,[41] R. Waldi,[62] C. Wallace,[48] R. Wallace,[12] J. Walsh,[23] S. Wandernoth,[11] J. Wang,[59] D. R. Ward,[47] N. K. Watson,[45] D. Websdale,[53] M. Whitehead,[48] J. Wicht,[38] D. Wiedner,[11] G. Wilkinson,[55] M. P. Williams,[45] M. Williams,[56] F. F. Wilson,[49] J. Wimberley,[58] J. Wishahi,[9] W. Wislicki,[28] M. Witek,[26] G. Wormser,[7] S. A. Wotton,[47] S. Wright,[47] S. Wu,[3] K. Wyllie,[38] Y. Xie,[61] Z. Xing,[59] Z. Xu,[39] Z. Yang,[3] X. Yuan,[3] O. Yushchenko,[35] M. Zangoli,[14] M. Zavertyaev,[10,u] L. Zhang,[59] W. C. Zhang,[12] Y. Zhang,[3] A. Zhelezov,[11] A. Zhokhov,[31] L. Zhong[3] and A. Zvyagin[38]

(LHCb Collaboration)

[1]*Centro Brasileiro de Pesquisas Físicas (CBPF) Rio de Janeiro, Brazil*
[2]*Universidade Federal do Rio de Janeiro (UFRJ) Rio de Janeiro, Brazil*
[3]*Center for High Energy Physics, Tsinghua University Beijing, China*
[4]*LAPP, Université de Savoie CNRS/IN2P3, Annecy-Le-Vieux, France*
[5]*Clermont Université Université Blaise Pascal, CNRS/IN2P3, LPC, Clermont-Ferrand, France*
[6]*CPPM, Aix-Marseille Université CNRS/IN2P3, Marseille, France*
[7]*LAL, Université Paris-Sud CNRS/IN2P3, Orsay, France*
[8]*LPNHE, Université Pierre et Marie Curie Université Paris Diderot, CNRS/IN2P3, Paris, France*
[9]*Fakultät Physik, Technische Universität Dortmund Dortmund, Germany*
[10]*Max-Planck-Institut für Kernphysik (MPIK) Heidelberg, Germany*
[11]*Physikalisches Institut, Ruprecht-Karls-Universität Heidelberg Heidelberg, Germany*
[12]*School of Physics, University College Dublin Dublin, Ireland*
[13]*Sezione INFN di Bari Bari, Italy*

[14]Sezione INFN di Bologna Bologna, Italy
[15]Sezione INFN di Cagliari Cagliari, Italy
[16]Sezione INFN di Ferrara Ferrara, Italy
[17]Sezione INFN di Firenze Firenze, Italy
[18]Laboratori Nazionali dell'INFN di Frascati Frascati, Italy
[19]Sezione INFN di Genova Genova, Italy
[20]Sezione INFN di Milano Bicocca Milano, Italy
[21]Sezione INFN di Milano Milano, Italy
[22]Sezione INFN di Padova Padova, Italy
[23]Sezione INFN di Pisa Pisa, Italy
[24]Sezione INFN di Roma Tor Vergata Roma, Italy
[25]Sezione INFN di Roma La Sapienza Roma, Italy
[26]Henryk Niewodniczanski Institute of Nuclear Physics Polish Academy of Sciences Kraków, Poland
[27]AGH-University of Science and Technology Faculty of Physics and Applied Computer Science, Kraków, Poland
[28]National Center for Nuclear Research (NCBJ) Warsaw, Poland
[29]Horia Hulubei National Institute of Physics and Nuclear Engineering Bucharest-Magurele, Romania
[30]Petersburg Nuclear Physics Institute (PNPI) Gatchina, Russia
[31]Institute of Theoretical and Experimental Physics (ITEP) Moscow, Russia
[32]Institute of Nuclear Physics, Moscow State University (SINP MSU) Moscow, Russia
[33]Institute for Nuclear Research of the Russian Academy of Sciences (INR RAN) Moscow, Russia
[34]Budker Institute of Nuclear Physics (SB RAS) and Novosibirsk State University Novosibirsk, Russia
[35]Institute for High Energy Physics (IHEP) Protvino, Russia
[36]Universitat de Barcelona Barcelona, Spain
[37]Universidad de Santiago de Compostela Santiago de Compostela, Spain
[38]European Organization for Nuclear Research (CERN) Geneva, Switzerland
[39]Ecole Polytechnique Fédérale de Lausanne (EPFL) Lausanne, Switzerland
[40]Physik-Institut, Universität Zürich Zürich, Switzerland
[41]Nikhef National Institute for Subatomic Physics Amsterdam, The Netherlands
[42]Nikhef National Institute for Subatomic Physics and VU University Amsterdam Amsterdam, The Netherlands
[43]NSC Kharkiv Institute of Physics and Technology (NSC KIPT) Kharkiv, Ukraine
[44]Institute for Nuclear Research of the National Academy of Sciences (KINR) Kyiv, Ukraine
[45]University of Birmingham Birmingham, United Kingdom
[46]H.H. Wills Physics Laboratory, University of Bristol Bristol, United Kingdom
[47]Cavendish Laboratory, University of Cambridge Cambridge, United Kingdom
[48]Department of Physics, University of Warwick Coventry, United Kingdom
[49]STFC Rutherford Appleton Laboratory Didcot, United Kingdom
[50]School of Physics and Astronomy, University of Edinburgh Edinburgh, United Kingdom
[51]School of Physics and Astronomy, University of Glasgow Glasgow, United Kingdom
[52]Oliver Lodge Laboratory, University of Liverpool Liverpool, United Kingdom
[53]Imperial College London London, United Kingdom
[54]School of Physics and Astronomy, University of Manchester Manchester, United Kingdom
[55]Department of Physics, University of Oxford Oxford, United Kingdom
[56]Massachusetts Institute of Technology Cambridge, Massachusetts, USA
[57]University of Cincinnati Cincinnati, Ohio, USA
[58]University of Maryland College Park, Maryland, USA
[59]Syracuse University Syracuse, New York, USA
[60]Pontifícia Universidade Católica do Rio de Janeiro (PUC-Rio) Rio de Janeiro, Brazil
(associated with Institution Universidade Federal do Rio de Janeiro (UFRJ) Rio de Janeiro, Brazil)
[61]Institute of Particle Physics, Central China Normal University Wuhan, Hubei, China
(associated with Institution Center for High Energy Physics, Tsinghua University Beijing, China)
[62]Institut für Physik, Universität Rostock Rostock, Germany
(associated with Institution Physikalisches Institut, Ruprecht-Karls-Universität Heidelberg Heidelberg, Germany)
[63]National Research Centre Kurchatov Institute Moscow, Russia
(associated with Institution Institute of Theoretical and Experimental Physics (ITEP) Moscow, Russia)
[64]Instituto de Fisica Corpuscular (IFIC) Universitat de Valencia-CSIC, Valencia, Spain
(associated with Institution Universitat de Barcelona Barcelona, Spain)
[65]KVI-University of Groningen Groningen, The Netherlands
(associated with Institution Nikhef National Institute for Subatomic Physics Amsterdam, The Netherlands)
[66]Celal Bayar University Manisa, Turkey (associated with Institution European Organization for Nuclear Research (CERN) Geneva, Switzerland)

[a]Also at Università di Firenze, Firenze, Italy.
[b]Also at Università di Ferrara, Ferrara, Italy.
[c]Also at Università della Basilicata, Potenza, Italy.
[d]Also at Università di Modena e Reggio Emilia, Modena, Italy.
[e]Also at Università di Padova, Padova, Italy.
[f]Also at Università di Milano Bicocca, Milano, Italy.
[g]Also at LIFAELS, La Salle, Universitat Ramon Llull, Barcelona, Spain.
[h]Also at Università di Bologna, Bologna, Italy.
[i]Also at Università di Roma Tor Vergata, Roma, Italy.
[j]Also at Università di Genova, Genova, Italy.
[k]Also at Universidade Federal do Triângulo Mineiro (UFTM), Uberaba-MG, Brazil.
[l]Also at AGH - University of Science and Technology, Faculty of Computer Science, Electronics and Telecommunications, Kraków, Poland.
[m]Also at Università di Cagliari, Cagliari, Italy.
[n]Also at Scuola Normale Superiore, Pisa, Italy.
[o]Also at Hanoi University of Science, Hanoi, Vietnam.
[p]Also at Università di Bari, Bari, Italy
[q]Also at Università degli Studi di Milano, Milano, Italy.
[r]Also at Università di Pisa, Pisa, Italy.
[s]Also at Università di Roma La Sapienza, Roma, Italy.
[t]Also at Università di Urbino, Urbino, Italy.
[u]Also at P.N. Lebedev Physical Institute, Russian Academy of Science (LPI RAS), Moscow, Russia.